DE GRUYTER J. Appl. Geodesy 2017; 11(1): 21–29

Tobias Kersten*, Martin Kobe, Gerald Gabriel, Ludger Timmen, Steffen Schön, and Detlef Vogel

Geodetic monitoring of subrosion-induced subsidence processes in urban areas

Concept and status report

DOI 10.1515/jag-2016-0029
Received July 1, 2016; accepted November 9, 2016

Abstract: The research project SIMULTAN applies an advanced combination of geophysical, geodetic, and modelling techniques to gain a better understanding of the evolution and characteristics of sinkholes. Sinkholes are inherently related to surface deformation and, thus, of increasing societal relevance, especially in dense populated urban areas. One work package of SIMULTAN investigates an integrated approach to monitor sinkhole-related mass translations and surface deformations induced by salt dissolution. Datasets from identical and adjacent points are used for a consistent combination of geodetic and geophysical techniques. Monitoring networks are established in Hamburg and Bad Frankenhausen (Thuringia). Levelling surveys indicate subsidence rates of about 4–5 *mm* per year in the main subsidence areas of Bad Frankenhausen with a local maximum of 10 *mm* per year around the leaning church tower.

Here, the concept of combining geodetic and gravimetric techniques to monitor and characterise geological processes on and below the Earth's surface is exemplary discussed for the focus area Bad Frankenhausen. For the different methods (levelling, GNSS, relative/absolute gravimetry) stable network results at identical points are obtained by the first campaigns, i.e., the results are generally in agreement.

Keywords: Co-located Geo-Monitoring, Sinkhole, Absolute and Relative Gravimetry, GNSS, Levelling, Earth's Surface Deformation

***Corresponding author: Tobias Kersten,** Leibniz Universität Hannover, Institut für Erdmessung, Schneiderberg 50, D-30167 Hannover, Germany, e-mail: kersten@ife.uni-hannover.de
Martin Kobe, Gerald Gabriel, Detlef Vogel, Leibniz Institute for Applied Geophysics (LIAG), Stilleweg 2, D-30655 Hannover, Germany, e-mails: martin.kobe@liag-hannover.de, gerald.gabriel@liag-hannover.de
Ludger Timmen, Steffen Schön, Leibniz Universität Hannover, Institut für Erdmessung, Schneiderberg 50, D-30167 Hannover, Germany, e-mails: timmen@ife.uni-hannover.de, schoen@ife.uni-hannover.de

1 Introduction

Sinkholes are circular to elliptical depressions or collapse structures at the Earth's surface, caused by subrosion processes, i.e., underground leaching of soluble rocks such as rock salt, anhydrite, or limestone. Diameters of sinkholes may range from a few metres to several hundred metres. Controlling factors are the local geological structure and the specific generation process as summarised in [27].

Especially in urban areas sinkholes are of societal relevance where they pose a severe hazard for infrastructure and life. The joint research project SIMULTAN (Sinkhole instability: integrated multi-scale monitoring and analysis) aims to develop and apply a system for early detection of sinkhole instabilities, unrests and collapses to gain deeper insight into these subsurface processes and related surface deformations. Concepts for monitoring, multi-scale description, and prediction of sinkhole evolution especially in urban areas are studied and applied since they are not yet fully developed. SIMULTAN focuses on aspects such as the understanding of interactions between surface and subsurface, the separation of different superimposing processes, as well as the prediction of future sinkhole development and the assessment of damage potential. In detail, the integrated approach is based on four scientific questions and methods:

1. Application of dedicated, high-resolution methods (e.g. seismics, geoelectrics, downhole logging, seismology, and direct-push methods) and inversion techniques to characterise structures, physical properties, and seismicity at different depth levels and scales.
2. Combination of geodetic (GNSS, levelling) and geophysical (relative and absolute gravimetry) measurements at identical and adjacent points to monitor deformation and mass changes on different spatio-temporal scales.
3. Interdisciplinary studies, time-dependent analyses, and joint interpretation of multiple data streams to derive process models, partly by improved modelling techniques.

4. Set up of an information platform to interpret measurements, to visualise information, and to evaluate case studies.

This paper addresses the second research topic, i.e., the joint application of geodetic and geophysical methods and the corresponding data integration.

SIMULTAN focuses on aspects such as the separation of different superimposed processes and the understanding of interactions between surface and subsurface, as well as the prediction of future sinkhole development and the assessment of damage potential. The research is performed on different scales with respect to time, lateral extent, and depth [13] and is designed to complement investigations and results from similar and related research projects [2, 6, 15, 18, 19, 20].

Target areas of SIMULTAN are located in Northern Germany and Thuringia, where the development of sinkholes is linked to salt structures [4]. In Central and Southern Germany the soluble rocks are mostly carbonates (Fig. 1, [26]). Hexagons in Fig. 1 represent evaporitic sinkhole formations that are targeted by SIMULTAN. The first area, Hamburg-Flottbek, is densely populated and slowly subsiding locally due to the leaching of the Othmarschen-Langenfelde salt diapir [4]. The second investigation area is Bad Frankenhausen, where sinkhole diameters are some tens of metres and which is discussed in more detail in this paper.

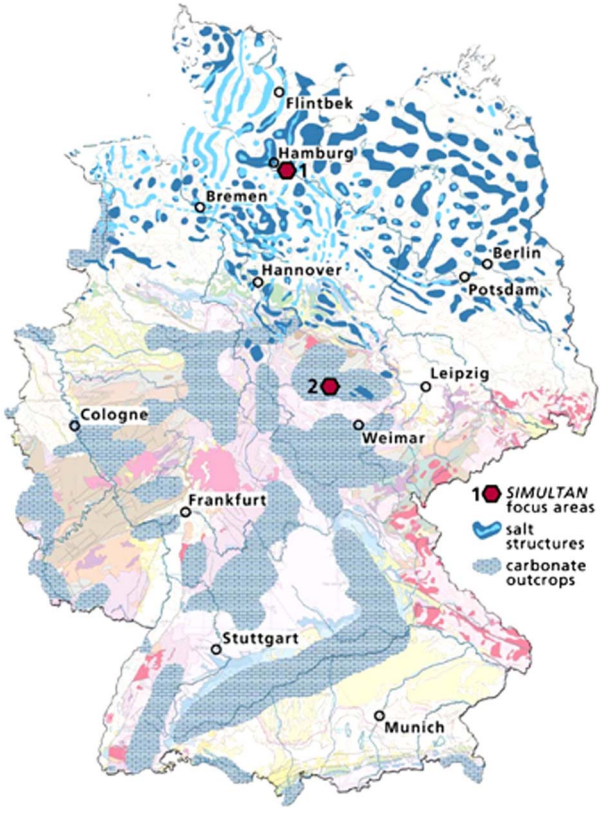

Figure 1: Simplified geological map of Germany that identifies regions of increased sinkhole hazard potential. Soluble rocks are commonly salt and carbonates. The two focus areas of the project SIMULTAN are also shown (after Krawczyk et al. [13]).

Several sinkholes have developed along the Kyffhäuser Southern Margin Fault and these processes are still ongoing. In Hamburg-Flottbek as well as Bad Frankenhausen the spatio-temporal evolution of surface deformation is still unknown in detail and an integrated interpretation of the data is missing. The geodetic work package in SIMULTAN combines geodetic and gravimetric surface monitoring techniques in close cooperation between the Leibniz Institute for Applied Geophysics (LIAG) and the Institut für Erdmessung (Leibniz Universität Hannover, LUH). This comprises absolute and relative gravimetry, levelling, and GNSS (GPS and GLONASS) campaigns.

The paper is organised as follows: section two presents the concept of the network and the monitoring strategy. Sections three and four address the geophysical and geodetic field measurements in detail. We will show that space geodetic and terrestrial geophysical and geodetic techniques are capable to detect even small displacements during the ongoing deformation monitoring in Bad Frankenhausen. Similar combinations of methods are already established in Hamburg Flottbek.

2 Concept and monitoring strategy

Surface deformation often consists of superimposed signals from several sources at different depths. The combination of classical geodetic and geophysical techniques, e.g., borehole extensometers, levelling instruments, gravimeters, and GNSS provides complementary information and allows to separate different sources [5, 14, 16].

In SIMULTAN, geophysical parameters of critical geological zones are resolved by monitoring vertical and horizontal surface displacement caused by mass relocations in the subsurface with different techniques at identical points. Precise GNSS and levelling campaigns are combined with gravimeter measurements at *identical* or *adjacent* points to study long periodic effects caused by subrosion processes that might be superimposed by seasonal effects. The term *integrated* describes a system characterisation in order to achieve an improved comprehensive solution from the joint interpretation of different kinds of results. Thus, *identical* or *adjacent* points are established

to perform co-located geo-monitoring with different sensors. Whenever possible the same marker is used to setup the instruments at the physically identical place; otherwise the instrumental reference points are linked by local ties. However, due to the urban conditions, sometimes not all of the used geodetic and geophysical techniques are combined at one identical measurement point. The derived key parameters are expected to become important results to assist and improve the modelling of rock-soil interaction in sinkhole formations and the subsurface cavity and collapse evolution [7, 9, 10, 11]. These studies are carried out by other groups in this joint research project. For numerical modelling, synthetic and most realistic models will be used both, the latter derived from geophysical and geological site surveys. Furthermore, the integration step comprises the forward-modelling and backward-evaluation between realistic datasets and related realistic model-prediction of the areas of interest.

2.1 Measurement points

The combination of various geodetic methods requires an observation network that is accessible for each of the used methods. The planning, selection, and installation of measurement points were carefully carried out. In Bad Frankenhausen they are located in active subsidence areas, e.g., around the leaning church tower, historical sinkholes, and in assumed stable areas to obtain clear evidence of gravity changes and vertical movements due to subsidence (cf. white bordered areas in Fig. 3). The gravimeter platforms GRAV2, GRAV11, and GRAV12, installed in January 2014, are concrete pillars, cast to reduce the influence of micro-seismic noise. They have a diameter of 0.30 *m*, a depth of 0.80 *m*, and a flat surface with north arrow (Fig. 2(b) and Fig. 5(d)). All other points are marked by 0.25 *m* long stainless steel tubes with a white cap and a fillister head.

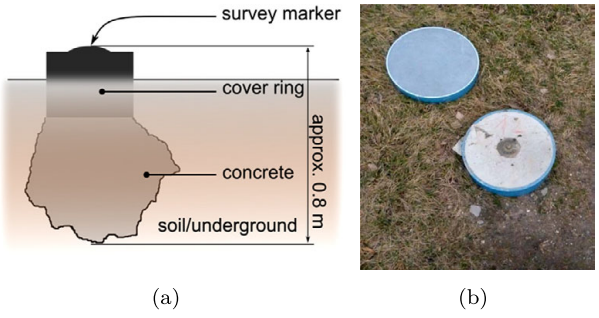

Figure 2: Measurement point as part of the monitoring network, (a) schematic sketch of the installation at some identical points in Bad Frankenhausen, (b) exemplarily for point GRAV12.

2.2 Monitoring network

The monitoring network in Bad Frankenhausen consists of about 120 points for precision levelling. Thirteen of these points define a local gravimetric network (Fig. 3) with two more distal gravity points outside the city serving as reference points (AP2 and AP4; Fig. 3). Precise levelling and gravimetric campaigns are conducted quarterly since March 2014 to gain time-lapse data sets. An absolute gravimeter point, as part of the control network, was established in 2015 to monitor the long-term stability of the gravity reference annually and thus, to identify regional gravity changes related to subrosion over several years or even decades.

The GNSS part of this multi-sensor monitoring network consists of six identical points (simultaneously used for gravimetry and levelling, Fig. 3) and two distal points (GGP1, SL03), where only GNSS is observed. Station SL03 serves as a local reference for the GNSS network. GNSS campaigns started in September 2015 and will be repeated every six months, closely aligned to the gravimeter and levelling campaigns. Additionally, the Geological Survey of Thuringia operates a borehole extensometer at GRAV7.

3 Levelling and gravimetry campaigns

The integrated study in SIMULTAN comprises monitoring at co-located points in quarterly (gravimetry, levelling) and semi-annually (GNSS) field campaigns, the combination and integration of the results of the different monitoring techniques, and their interpretation as an integrated solution.

The levelling network of about 120 points was established to observe subsidence in the northern area of the city and to provide evidence for measuring campaigns using GNSS. Furthermore, levelling supports the processing and interpretation of the gravity data by providing heights and height changes for different processing steps, e.g., further gravity anomaly calculation.

Levelling campaigns are performed with Leica Geosystems digital levels DNA03 and bar code invar staffs (manufacturer accuracy information: $\pm 0.3\,mm$ per $1\,km$ of double levelling). The obtained standard deviation for one km of double levelling is in the range of 1.5 *mm* or less in each of

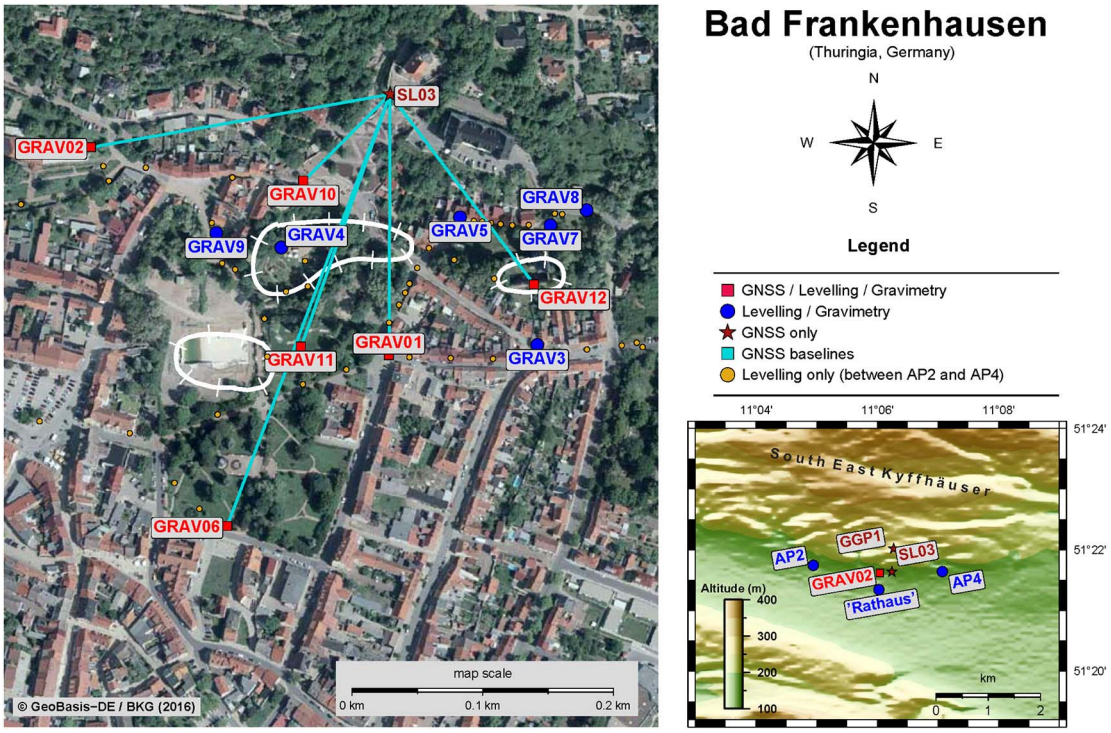

Figure 3: Location of GNSS and co-located points as part of the geodetic monitoring network in Bad Frankenhausen; white bordered areas indicate regions of recent sinkhole events.

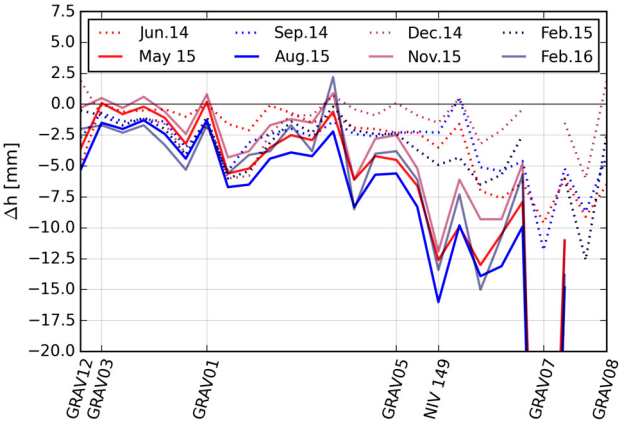

Figure 4: Subsidence from March 2014 (baseline reading; black line) to February 2016 obtained from quarterly performed precise levellings. Graphs are based on all levelling points along a profile, that starts at GRAV12 and ends at GRAV8 (cf. Fig. 3). At GRAV7 subsidence amounts to ca. 70 *mm*, but is expected to be partially induced by construction work.

the nine field campaigns. Furthermore, the results reveal an annually maximum subsidence rate of around 4–5 *mm* in the main subsidence areas and about 10 *mm* around the leaning church tower since 2014 (Fig. 4). The significantly higher values observed on the profile between the points GRAV5 and GRAV8 can possibly be explained by compaction of the soil due to extensive construction work near point GRAV7. It is not yet possible to separate these effects from long-term, subrosion-induced subsidence. Thus, the observed trend must be confirmed by forthcoming campaigns and, hence, the signals are not taken into account for this evaluation.

3.1 Gravimetry

A brief overview on relative and absolute gravity is given by Timmen [22]. During every relative gravimetry campaign four different gravimeters of the types Scintrex CG3, CG5, and LaCoste & Romberg (LCR) are used to optimise the network surveys. In total, 15 gravity points (13 local and 2 distant reference points) are observed using the step method for drift control of the spring gravimeters [25].

Data processing includes the elimination of outliers, jumps, and other failures in the data sets as well as the reduction for earth tides, different instrument heights and air mass redistributions. Moreover, calibration and the sealing of the sensors against instrumental air pressure effects are checked regularly. Inside the local observation area, the maximum gravity difference is $44.5\,\mu m\,s^{-2}$ between the points GRAV4 and GRAV12, hence, a calibration accuracy of better than 10^{-3} ($\approx 0.0445\,\mu m\,s^{-2}$) is re-

Table 1: Results of the absolute gravimetry campaign with the gravity meter FG5X-220 on the *Rathaus* point (cellar vault, Fig. 5(a)).

Point Rathaus	Measurement run (orientation)	Date in 2015	Drops	$\delta g/\delta h$ [$\mu m\,s^{-2}\,m^{-1}$]	$g_{h=1.25}$ [$\mu m\,s^{-2}$]	$g_{h=0.00}$ [$\mu m\,s^{-2}$]
Setup 1	20150622a (N)	June, 22.–23.	988	−2.678	9811717.488	
Setup 2	20150623a (W)	June, 23.–24.	798	−2.678	9811717.458	
Average		June, 22.–24.	1796	−2.678	9811717.473	9811720.820

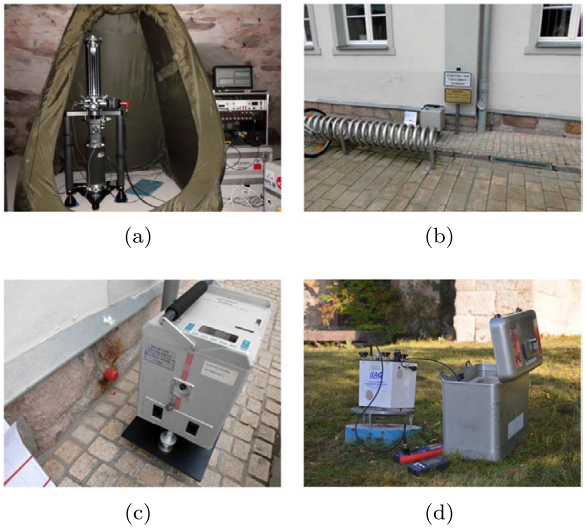

(a) (b) (c) (d)

Figure 5: Relative and absolute gravimeter measurements at Bad Frankenhausen. Absolute gravity value determined with FG5X-220 in cellar vault (a), determination of local gravity tie from absolute to relative point using levelling mark as survey station (b, c), and relative measurements with LaCoste&Romberg-Gravimeter (LCR) on GRAV12 (d).

quired to avoid significant systematic effects on the whole network. The obtained standard deviations of the gravity points in each campaign are less than $0.02\,\mu m\,s^{-2}$ (Scintrex), $0.05–0.07\,\mu m\,s^{-2}$ (LCR). For a combined adjustment of the data from all gravimeters, they are in the order of $0.015\,\mu m\,s^{-2}$ or even better.

The absolute gravimeter point was established in Bad Frankenhausen in June 2015 to determine and control the absolute gravity level (datum) for the relative gravimetry campaigns. The absolute gravity point is located in the basement of the town hall of Bad Frankenhausen. Measurements were performed by LUH using the Hannover absolute gravimeter FG5X-220 (Fig. 5(a)). This gravimeter participated in the latest international comparisons (Walferdange, Luxembourg, Nov. 2013 and Belval, Luxembourg, Nov. 2015) and agrees within a few $0.015\,\mu m\,s^{-2}$ with the international realised measuring level, cf. [23]. The results are shown in Table 1. Earth tides were reduced [24] and atmospherically induced gravity changes were considered by applying a correlation factor of $3.0\ nm\,s^{-2}\,hPa^{-1}$. The gradient-insensitive sensor height depends on the gravimeter setup and is close to $1.25\,m$ above floor level. Thus, the reference height $h = 1.25\,m$ (above floor point) was chosen for comparison reasons. The applied vertical gradient is assumed to be constant along the plumb line at this point and, because of the chosen reference height, the effect of its uncertainty on the absolute value can be neglected. The gradient $\delta g/\delta h$ was measured with the Scintrex CG3M-4492 gravimeter of LUH between the sensor positions $0.251\,m$ and $1.165\,m$ above floor point. The observed gravity gradient was determined to $-2.678\,\mu m\,s^{-2}$ per m with a standard deviation of $0.010\,\mu m\,s^{-2}$ per m. To support relative gravimetric measurements, the centred g-value ($h = 0.000\,m$) is also provided in Table 1.

The local tie between the basement-located absolute gravity point and the levelling mark (cf. Fig. 5(c)) in front of the town hall (simultaneously the starting point of relative gravimetry) was determined using the CG3M-4492. The determined Δg-value between the absolute and relative point is $\Delta g = 4.631\,\mu m\,s^{-2}$ with a standard deviation of $\sigma_{\Delta g} = 0.015\,\mu m\,s^{-2}$.

4 GNSS campaigns

For consistent monitoring, equal or very similar GNSS receivers (Leica GRX1200+GNSS, GRX1200GG Pro and GX1230GG) with GPS and GLONASS capability are used. Local reference stations and challenging stations are equipped with 3D choke ring antennas (Leica AR25 Rev. 3) to mitigate most of expectable multipath. All other stations are equipped with rover antennas for economic reasons. The used GNSS antennas were absolutely calibrated at the LUH facility using the robot based approach [21, 29]. Additionally to the horizontal components, the height component is of particular interest. Therefore, the special tripod adaptor FG-ANA100B (ref. Fig. 6) is used in SIMULTAN campaigns. This tripod, in combination with the near-field calibrated carrier phase center corrections (PCCs), is used for high-precision GNSS levelling surveys [8]. The adaptor

(a) (b)

Figure 6: GNSS adaptor for precise GNSS height levelling, (a) mockup for calibration on robot and (b) installation in the field with 50 *cm* scale beneath the ARP exemplarily shown for point GRAV12.

contains a 0.5 *m* scale, directly connected to the antenna reference point (ARP), enabling a precise and contactless determination of the antenna height during the GNSS sessions.

4.1 Session setup

Each GNSS campaign consists of three sessions of four hours. Data is recorded with one second interval (internal purposes) but processed with ten seconds to adjust the final GNSS network.

To meet the requirements of a stable and reliable local reference station, we decided to use SL03 (indicated by a red star in Fig. 3), a concrete pillar with well-defined centring that is also part of another monitoring network. Along with the point GRAV11, the local reference is observed continuously during all 6 sessions. A star-like network is formed for each campaign with baselines starting at SL03. GNSS stations with square symbol in Fig. 3 are occupied during three sessions.

4.2 Campaign preparation

Concerning GNSS, there are two challenges in SIMULTAN. First, the horizontal and vertical components should be accurate in order to determine even small deformation. Second, urban environments are challenging for a stable acquisition of GNSS signals due to signal obstructions, multipath, and diffractions. Detailed station analysis verified moderate obstructions in the field of view for the receiving antennas at all selected GNSS points. Additional studies are focused on adaptive and dynamic elevation masks that will improve the signal availability and stabilise the ambiguity resolution.

A zero baseline (ZB) test at the laboratory network of LUH examines the expectable performance of the used GNSS equipment and delivers quality parameters for:

1. Achievable carrier-to-noise ratio (C/N_0) for receiver-antenna combination under ordinary campaign settings; cf. Fig. 7, [1] and determination of nominal C/N_0 curves.
2. Analysis of double differences (DD) between the individual receivers.

The obtained DDs prove a noise level with peak-to-peak variations of $\pm 3.5\,mm$. The C/N_0 values are adequate to quantify the signal quality. Following Brunner et al. [1] C/N_0 reference curves are necessary to describe the nominal behaviour of the receiver-antenna combination. Reference curves can be evaluated using a moderate amount of satellite observations in a static approach with few obstructions (Fig. 7(a)) or by antenna calibration with a robot [12, 17]. Fig. 7(a) summarises C/N_0 values for all measured satellites during 24 hours w.r.t. the elevation in the antenna's body frame. At elevations between 30°–90° stable C/N_0 of 52 *dB-Hz* are observed. At elevations lower than 30° a continuously decreasing of the C/N_0-values down to 42 *dB-Hz* are apparent. In contrast to Fig. 7(a), where a typical C/N_0 curve from the ZB test is shown, C/N_0 values of a four hours session at point GRAV12 are depicted in Fig. 7(b). There, large C/N_0 deviations from the nominal curve (black line) are detectable for observations below 45°. These effects are induced by signal diffraction and subsequently distorted carrier phase observations.

The processing of the GNSS network is performed using Bernese 5.2 [3] and ESA (European Space Agency) products, e.g., clock, orbits, earth rotation parameters and differential code biases.

Advanced station analysis (study of dynamic and adaptive elevation masks, DD analysis on the observed-minus-computed level (OMC)), is performed using the GNSS MATLAB Toolbox, that is developed at LUH [28].

4.3 Network solution

The network processing was evaluated using both a GPS only and a GPS/GLONASS combined solution to study the impact on the network performance.

Final results of the first GNSS campaign are summarised in Fig. 8 and prove the valuable improvement for the combined solution. Especially the height component is much more reliable but also the repeatability for the horizontal component is improved. Gaining an optimal estimate for the height component is a challenge due to sev-

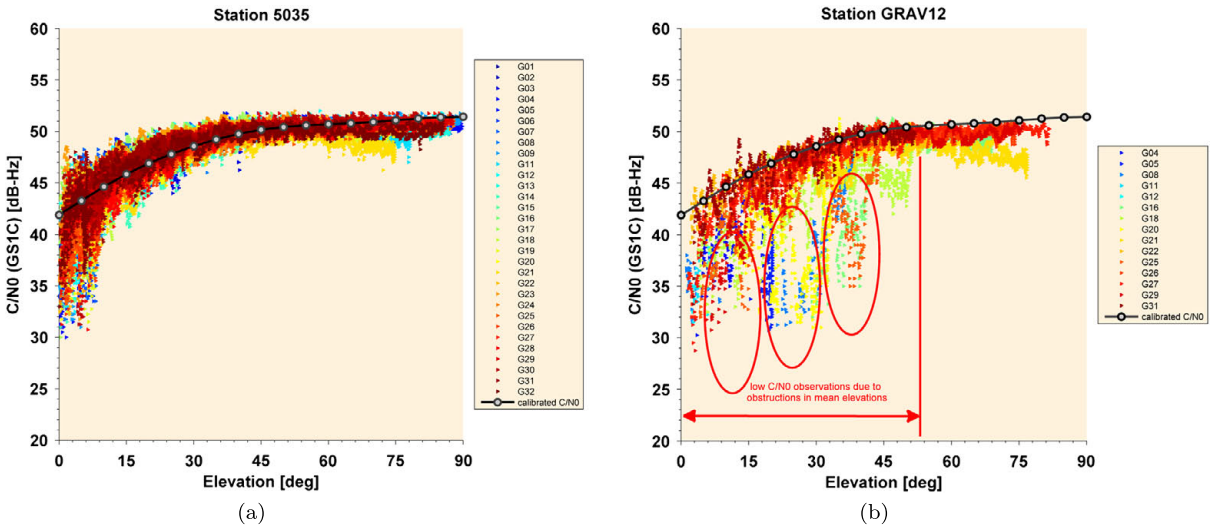

Figure 7: Carrier-to-noise density ratio (C/N_0) as signal quality indicator, (a) Determination of a nominal behaviour at the laboratory network of LUH, and (b) observed C/N_0 in Bad Frankenhausen with the same antenna/receiver combination but influenced by urban reflectors.

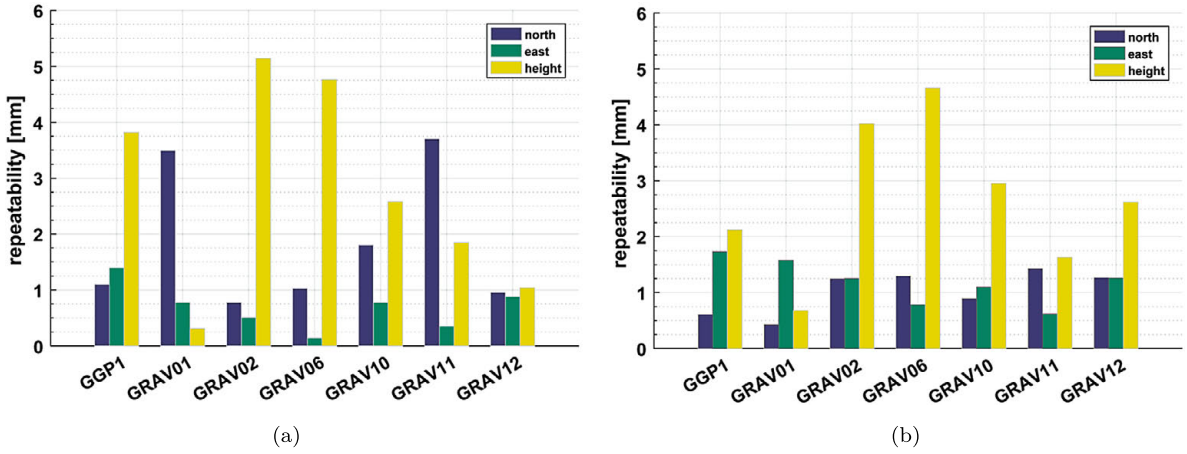

Figure 8: Repeatability of GNSS monitoring network solution, (a) GPS only, (b) GPS and GLONASS combined solution.

eral urban reflectors and obstructions. The advantage of GLONASS is the higher inclination of the orbital planes. Subsequently, especially the northern hole (a characteristic at mid-latitudes) can be reduced. Furthermore, the double amount of observations stabilises the result.

First studies concerning the usage of adaptive and dynamic elevations masks show that their application stabilises the position repeatability, so that satellite arcs with interrupted and disturbed observations are identified and reduced to a minimum. The quality of the obtained data is improved, since deficiencies of satellite visibility are strongly related to azimuth and elevation of the incoming satellite signal.

Table 2 evaluates the GNSS and levelling heights against each other with the NHN (Normal Heights; German Height System 1992) from the latest levelling campaign, carried out in September 2015 (hence, temporally close to the GNSS campaign). The point GRAV10 is chosen as reference, since this point represents the medium repeatability for all GNSS-heights (cf. Fig. 8). The last column of Table 2 validates differences of relative heights derived from GNSS and levelling. Results are comparable to each other at the $\pm 3\,mm$ level with exception of GRAV12. Thus, an accuracy of the urban-located GNSS monitoring network in the order of 2–3 *mm* (cf. Fig. 8 and Tab. 2) is proven. However, unavoidable challenging observation conditions (like at point GRAV12 where a high wall is located in close vicinity to the point in the north) can deteriorate the performance yielding height differences of 4.7 *mm*. Therefore, further studies on adaptive and dynamic elevation masks and multipath mitigation will be carried out to further improve the results.

Table 2: Comparison of relative GNSS and levelling height differences.

Number	Name	NHN92 Height [m]	GNSS Height [m]	Δ Levelling [m]	Δ GNSS [m]	Δ GNSS − Δ Levelling [mm]
1	GRAV1	140.2861	185.8377	−1.0373	−1.0386	−1.3
2	GRAV2	143.7469	189.2970	2.4235	2.4207	−2.8
3	GRAV6	132.7434	178.2935	−8.5800	−8.5828	−2.9
4	GRAV10	141.3234	186.8763	0.0000	0.000	0.0
5	GRAV11	140.2651	185.8193	−1.0583	−1.0570	1.3
6	GRAV12	152.9325	198.4901	11.6091	11.6138	4.7

5 Summary and outlook

First results from the geodetic campaigns within SIMULTAN to monitor sinkholes in Bad Frankenhausen are shown. The established network consists of 120 levelling points. Fifteen of these points are used in a gravity network, whereof six points are additionally occupied by GNSS. The first multi-sensor monitoring campaigns were performed. Quarterly levelling confirms an annually subsidence rate of 4–5 *mm* in the main subsidence areas that reaches a local maximum of 10 *mm*. The quarterly observed gravity network covers a gravity range of $44.5\,\mu m\,s^{-2}$ between the points GRAV4 and GRAV12. In addition, annual monitoring of the absolute gravity reference has been initiated by LUH in 2015 deploying the FG5X-220 free-fall gravimeter.

Semi-annually GNSS campaigns were evaluated and are ongoing. In contrast to a single GPS processing, the GNSS solution provides improved estimates for the horizontal and height component of 2–3 *mm* for optimal points and up to 5 *mm* in the horizontal components and 5–6 *mm* in the height components for challenging stations.

Urban sites are a challenge for all kind of applied measurement techniques, but we show that reliable solutions are feasible. Additional campaigns will be conducted to achieve and improve our understanding of land subsidence. Moreover we intend to evaluate the potential of InSAR to complement the monitoring concept.

Acknowledgment: The authors thank the TLVerm Thuringia, Glückauf Vermessung GmbH Sondershausen, and the city of Bad Frankenhausen for their kind cooperation. Furthermore, we thank the LGLN (Lower Saxony) for providing additional FG ANA100B GNSS height adaptors and corresponding accessories. The European Space Agency (ESA) is thanked for providing freely GNSS products.

Funding: This work package of SIMULTAN is funded under the grants 03G0843A and 03G0843D by the Bundesministerium für Bildung und Forschung, based on a resolution by the German Bundestag.

References

[1] Brunner, F. K., Hartinger, H., and Troyer, L. (1999). GPS signal diffraction model: the stochastic SIGMA-d model. *Journal of Geodesy*, 73:259–267.

[2] Camitz, J., Sigmundsson, F., Jahn, C.-H., Völksen, C., and Einarsson, P. (1995). Plate boundary deformation and continuing deflation of the Askja volcano, North Iceland, determined with GPS, 1987–1993. *Bulletin of Volcanology*, 57:136–145.

[3] Dach, R., Lutz, S., Walser, P., and Fridez, P., editors (2015). *Bernese GNSS Software Version 5.2*. University of Bern. User manual of the Bernese GNSS Software, Version 5.2.

[4] Dahm, T., Heimann, S., and Bialowons, W. (2011). A seismological study of shallow weak micro-earthquakes in the urban area of Hamburg city, Germany, and its possible relation to salt dissolution. *Natural Hazards*, 58(3):1111–1134.

[5] Foulger, G. R., Jahn, C.-H., Seeber, G., Einarsson, P., Julian, B. R., and Heki, K. (1992). Post Rifting Stress Relaxation at the Accretionary Plate Boundary in Iceland Measured Using Global Positioning System (GPS). *Nature*, 358:488–490.

[6] Fuhrmann, T., Heck, B., Knöpfler, A., Masson, F., Mayer, M., Ulrich, P., Westerhaus, M., and Zippelt, K. (2012). Recent surface displacements in the Upper Rhine Graben – Preliminary results from geodetic networks. *Tectonophysics*, 602:300–315.

[7] Hiller, T., Kaufmann, G., Romanov, D., and Gabrovsek, F. (2012). Formation of large collapse dolines: A three-dimensional numerical perspective. In *EGU General Assembly*, 2012, April 22–27, Vienna, Austria, page 1604.

[8] Hirt, C., Schmitz, M., Feldmann-Westendorff, U., Wübbena, G., Jahn, C.-H., and Seeber, G. (2010). Mutual validation of GNSS height measurements and high-precision geometric-astronomical leveling. *GPS Solutions*, 15(2):149–159.

[9] Holohan, E. P., Walter, T. R., Schöpfer, M. P., Walsh, J. J., van Wyk de Vries, B., and Troll, V. R. (2013). Origins of oblique-slip faulting during caldera subsidence. *Journal of Geophysical Research*, 118(4):1778–1794.

[10] Kaufmann, G., Romanov, D., and Hiller, T. (2010). Modelling three-dimensional karst aquifer evolution using different matrix-flow contributions. *Journal of Hydrology*, 388(3–4):241–250.

[11] Kaufmann, G., Romanov, D., and Nielbock, R. (2011). Cave detection using multiple geophysical methods: Unicorn cave, Harz Mountains, Germany. *Geophysics*, 76(3):71–76.

[12] Kersten, T. and Schön, S. (2012). *Von der Komponentenkalibrierung zur Systemanalyse: Konsistente Korrekturverfahren von Instrumentenfehlern für Multi-GNSS – Schlussbericht zum BMBF/DLR Vorhaben 50NA0903*. Technische Informationsbibliothek Hannover (TIB). http://edok01.tib.uni-hannover.de/edoks/e01fb02/359009840.pdf.

[13] Krawczyk, C. M., Polom, U., and Buness, H. (2015). Geophysikalische Schlüsselparameter zur Überwachung von Erdfällen – Stand und Ziele der aktiven Seismik. In Gesellschaft, D. G., editor, *DGG-Kolloquium Georisiken, Erdfälle*, pages 19–29. Special Issue I/2015.

[14] NAM (2000). *Bodemdaling door Aardgaswinning Groningen veld en randvelden in Groningen, Noord Drenthe en het Oosten van Friesland – Status Rapport en Prognose tot het jaar 2050*. Unpublished report. Nederlandse Aardolie Maatschappij BV.

[15] Pringle, J. K., Styles, P., Howell, C. P., Branston, M. W., Furner, R., and Toon, S. M. (2012). Long-term time-lapse microgravity and geotechnical monitoring of relict salt mines, Marston, Cheshire, U.K. *Geophysics*, 77(6):B287–B294.

[16] Rajiyowiryono, H. (1999). Groundwater and land subsidence monitoring along the north coastal plain of Java island. *CCOP Newsletter*, 24(3):19.

[17] Rao, B. R., Kunysz, W., Fante, R. L., and McDonals, K. (2013). *GPS/GNSS Antennas*. Artech House Publishers, Norwood, USA.

[18] Reuther, C., Buurmann, N., Kühn, D., Ohrnberger, M., Dahm, T., and Scherbaum, F. (2007). Erkundung des unterirdischen Raums der Metropolregion Hamburg – Das Projekt HADU. *Geotechnik: Organ der Deutschen Gesellschaft für Geotechnik*, 29(1):11–20.

[19] Schmidt, S., Wunderlich, J., Peters, A., and Heinke, O. (2013). Ingenieurgeologische Erkundung des Erdfalls vom 01. Nov. 2010 am Rötbergrain in Schmalkalden und Beschreibung des Erdfallfrühwarnsystems in Schmalkalden. Technical report, Thür. Landesanst. f. Umwelt und Geologie.

[20] Schmidt, W. (2005). *Geological and geotechnical investigation procedures for evaluation of the causes of subsidence damage in Florida*. Number 57. Florida Geological Survey, Division of Resource Assessment and Management, Tallahassee, Florida. Special Publication.

[21] Seeber, G. and Böder, V. (2002). Entwicklung und Erprobung eines Verfahrens zur hochpräzisen Kalibrierung von GPS Antennenaufstellungen – Schlussbericht zum BMBF/DLR Vorhaben 50NA9809/8. *Institut für Erdmessung*.

[22] Timmen, L. (2010). Absolute and relative gravimetry. In Xu, G., editor, *Sciences of Geodesy – I*, pages 1–48. Springer, Berlin/Heidelberg.

[23] Timmen, L., Engfeldt, A., and Scherneck, H.-G. (2015). Observed secular gravity trend at Onsala station with the FG5 gravimeter from Hannover. *Journal of Geodetic Sciences*, 5(1):18–25.

[24] Timmen, L. and Wenzel, H.-G. (1995). Worldwide Synthetic Gravity Tide Parameters. In Sünkel, H. and Marson, I., editors, *Gravity and Geoid: Joint Symposium of the International Gravity Commission and the International Geoid Commission*, pages 92–101. Springer Berlin Heidelberg, Berlin/Heidelberg.

[25] Torge, W. and Müller, J. (2012). *Geodesy*. De Gruyter, Berlin/Boston, 4th edition.

[26] Wadas, S. H., Polom, U., and Krawczyk, C. M. (2016). High-resolution shear-wave seismic reflection as a tool to image near-surface subrosion structures – a case study in Bad Frankenhausen, Germany. *Solid Earth*, 7:1491–1508.

[27] Waltham, T., Bell, F. G., and Culshaw, M. (2005). *Sinkoles and Subsidence*, volume Geophysical Sciences. Springer. DOI: 10.1007/b138363.

[28] Weinbach, U. and Schön, S. (2011). GNSS receiver clock modeling when using high Precision oscillators and its impact on PPP. *ASR*, 47(2):229–238. DOI: 10.1016/j.asr.2010.06.031.

[29] Wübbena, G., Menge, F., Schmitz, M., Seeber, G., and Völksen, C. (1997). A New Approach for Field Calibration of Absolute GPS Antenna Phase Center Variations. *Navigation*, 44(2):247–255.